

CHAPTER 3

^1H NMR Studies of Ru(phen)(bpy')(dppz) $^{2+}$ Covalently Tethered to a DNA

Abstract

^1H NMR spectroscopy was employed in structural studies of three ligand ruthenium complex $[\text{Rh}(\text{phen})(\text{bpy}')(\text{dppz})]^{2+}$ tethered covalently to a carefully designed short eightmer duplex via a nine carbon linker. Control NMR experiments were performed with two other constructs: a) the eightmer duplex containing covalently bound nine carbon linker, and b) the eightmer duplex. Issues of intercalation, exchange rate and binding site have been explored. Fast exchange in the timescale of the NMR experiments was observed at all the conditions in case of the oligonucleotide tethered to the metal complex. Comparison of the NOESY data among the control samples led us to conclude that the nine carbon linker is positioned between the second and fourth bases of the complementary strand. Due to the fast exchange in case of the metal tethered duplex, detailed structural information could not be obtained from this system.

Introduction

There is a wealth of activity and interest in understanding and developing the DNA binding properties of ruthenium(II) polypyridyls (1-6). The luminescent characteristics of ruthenium complexes and their perturbations on binding to DNA have led to their general application as spectroscopic probes for nucleic acids. Among these intercalators, $[\text{Ru}(\text{phen})_2\text{dppz}]^{2+}$ (phen = 1,10 phenanthroline; dppz = dipyrido[3,2-a:2',3'-c]phenazine) has shown the most promise in diagnostic applications which target nucleic acids (1-6). Quenched in aqueous solution, $[\text{Ru}(\text{phen})_2\text{dppz}]^{2+}$ luminesces brightly when intercalated into DNA. This luminescent characteristic, coupled with high binding affinity for DNA ($K_a \approx 10^6 \text{ M}^{-1}$) permits the application of $[\text{Ru}(\text{phen})_2\text{dppz}]^{2+}$ as a nonradioactive probe of double-stranded DNA at analytical concentrations. Dppz complexes of Os(II) (7) and Re(I) (8) have also been prepared and show DNA-dependent luminescence with distinct spectroscopic characteristics. Importantly, the luminescence of the dppz complexes appear to be quite sensitive to the geometry of stacking between the dppz ligand and DNA base pairs. $\text{Ru}(\text{phen})_2(\text{dppz})^{2+}$ has also been extensively utilized to study fast long-range electron transfer that is mediated by the stacked bases of DNA (9). In last few years, $\text{Ru}(\text{phen})(\text{bpy}')(\text{dppz})^{2+}$ ($\text{bpy}' = 4\text{-butyric acid-4'-methylbipyridine}$) tethered covalently to oligonucleotides has been employed extensively for long-range electron transfer studies and luminescence and EPR experiments (10). As the ruthenium (II) polypyridyl complexes have a wide range of applications that are dependent upon their ability to bind DNA by intercalation, it is important that a detailed description of their DNA binding specificity and intercalation geometry be established. Hence it becomes essential to develop a structural understanding of the intercalation of dppz complexes in DNA.

Despite wide interest in these complexes, there is currently not much information concerning DNA site-specificity and intercalative geometries of dppz complexes,

particularly where the dppz complexes are tethered covalently to the duplexes. To date, most of what is known about non-covalent $[\text{Ru}(\text{phen})_2\text{dppz}]^{2+}$ -DNA interactions originates from results obtained using luminescence (2, 6-8, 11), and NMR spectroscopy (12). $[\text{Ru}(\text{phen})_2\text{dppz}]^{2+}$ complexes bound to DNA display a biexponential decay in emission (2). Studies of asymmetrically substituted $[\text{Ru}(\text{phen})_2\text{dppz}]^{2+}$ derivatives (6), differential quenching experiments using hydrophobic and polar proton transfer quenchers (11), as well as luminescence studies using a range of nucleic acids, all support models for two intercalative geometries. In the first model, the dppz ligand may intercalate in a head-on fashion with the long axis of the dppz ligand parallel to the dyad axis of the base pair. In this orientation, both phenazine nitrogens are well protected. In the second proposed orientation, these axes may form an acute angle, maximizing stacking with the base pair and producing a canted geometry in which one side of the ligand is more exposed to solvent than the other. From NMR studies, it was proposed that $\text{Ru}(\text{phen})_2(\text{dppz})^{2+}$ intercalates from the major groove (12). Moreover, from the chemical shifts of dppz ligand proton resonances upon binding to DNA, it was suggested that $\text{Ru}(\text{phen})_2(\text{dppz})^{2+}$ isomers bind to the DNA helix with a population of intercalative geometries consistent with earlier structural models based upon luminescence studies. However, a fundamental problem in the NMR studies in case of the non-covalently bound $\text{Ru}(\text{phen})_2(\text{dppz})^{2+}$ was the lack of site specificity of the metal complex in DNA.

In all these studies (12), the metal complex binds in relative fast to intermediate exchange in the time scale of the NMR thereby, making it difficult to extract detailed and meaningful information from those experiments. One interesting way to get around this problem of lack of site specificity is to induce artificial site specificity in the metal complex by linking it to the DNA by a covalent linker. The length of the linker will limit the “zone” of intercalation of the metal complex, thereby possibly making it more site specific than its non-covalently bound counterparts enabling more detailed structural study of these systems.

Towards that goal in mind, we have attempted a thorough ^1H NMR study of a model system of a short eightmer duplex tethered to $\text{Ru}(\text{phen})(\text{bpy}')(\text{dppz})^{2+}$ by a nine-carbon linker. This assembly of nine-carbon linker and the metal complex was extensively used in spectroscopic and long-range charge transport studies.

Experimental Section

Oligonucleotide Design. Obtaining meaningful ^1H NMR structural information about the three ligand metal complex bound to a duplex calls for careful design and planning of the experiment. The plan is to use three constructs (Figure 1) employing an unmodified duplex (a), a duplex modified with the nine carbon linker (b) and finally the duplex tethered to $\text{Ru}(\text{phen})(\text{bpy}')(\text{dppz})^{2+}$ (c). The sequence of the duplex is carefully chosen so that it has higher probability of obtaining a well resolved NMR spectra with base aromatic proton resonances as less overlapping as possible.

Oligonucleotide Preparation. The oligonucleotides (8 base pairs) were synthesized using standard phosphoramidite chemistry on an Applied Biosystems 392 DNA synthesizer with a dimethoxy trityl protective group on the 5' end (13). Oligonucleotides were purified on a reversed-phase Rainin Dynamax C_{18} column on a Waters HPLC and deprotected by incubation in 80% acetic acid for 15 min. After deprotection, they were purified again by HPLC. The concentration of the oligonucleotides was determined by UV-visible spectroscopy (Beckman DU 7400), using the extinction coefficients estimated for single-stranded DNA, $\epsilon(260 \text{ nm}, \text{M}^{-1} \text{ cm}^{-1})$: adenine (A) = 15 400, inosine (I) = 11,000, guanine (G) = 11 500, cytosine (C) = 7400, and thymine (T) = 8700. Single strands were mixed with equimolar amounts of the complementary strands and were annealed in a Perkin-Elmer Cetus Thermal Cycler by gradual cooling from 90°C to ambient temperature in 90 min.

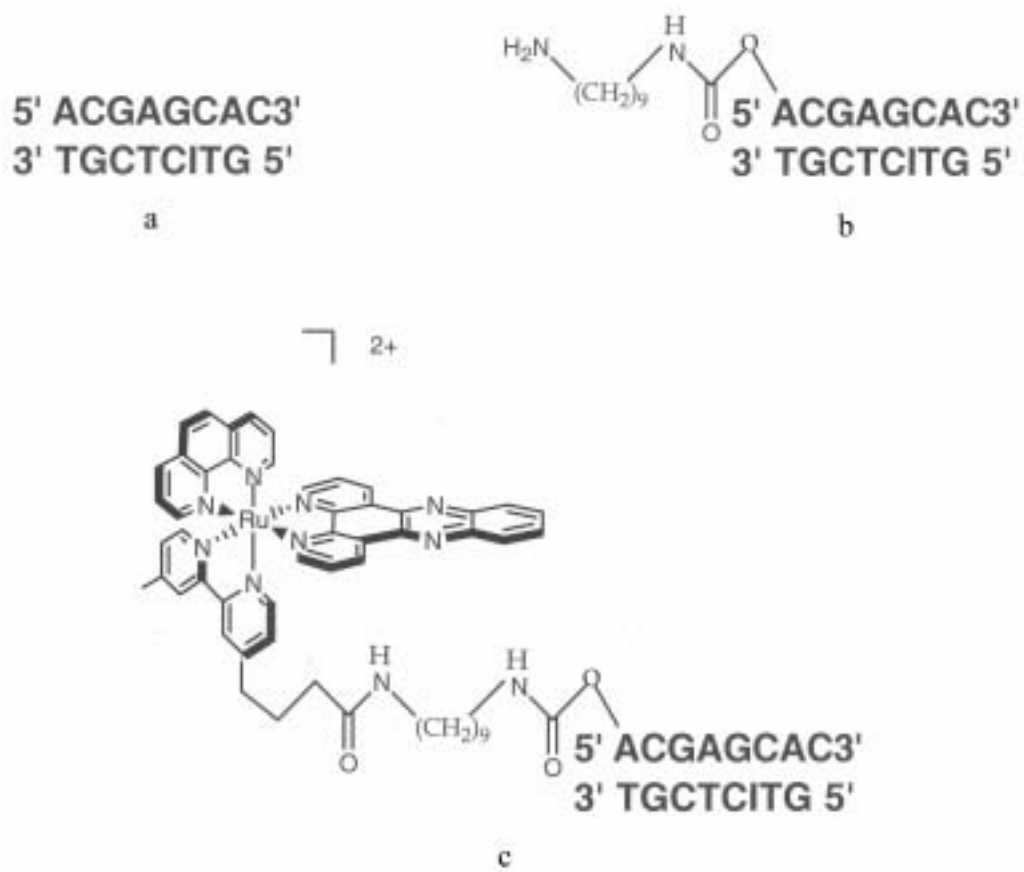


Figure 3.1. Constructs employed in the NMR study of three ligand ruthenium complex tethered to DNA. Shown are (a) the unmodified duplex, (b) a duplex modified with the nine carbon linker, (c) and the duplex tethered to Ru(phen)(bpy')(dppz)²⁺.

Synthesis of the Ruthenium Complex. Ru(phen)(bpy')(dppz)²⁺ (phen = 1,10 phenanthroline; bpy' = 4-butyric acid-4'-methylbipyridine; dppz = dipyrido[3,2-a:2',3'-c]phenazine) was prepared according to published procedures (14).

Preparation of Ruthenium and Linker-Modified Oligonucleotides.

Ruthenium-tethered 8-base-pair oligonucleotide and linker modified oligonucleotide were prepared according to published procedures (15, 16) and purified on a reversed-phase Rainin Dynamax C₁₈ column on a Hewlett-Packard 1050 HPLC. We were unable to resolve the diastereomers of ruthenium modified oligonucleotide, despite using a variety of column and HPLC eluent conditions, possibly because of relative short length of the metal complex modified duplex. The ruthenium-conjugated oligonucleotide was quantitated using the following extinction coefficient: for Ru(phen)(bpy')(dppz)²⁺ modified oligonucleotides, $\epsilon(432 \text{ nm}, \text{M}^{-1} \text{ cm}^{-1}) = 19,000$, while the linker modified oligonucleotide was quantified as unmodified oligonucleotide. Both the modified oligonucleotides were characterized by MALDI mass spectrometry (Figure 2). The calculated M.W. closely matches that obtained from the experimental results.

Sample Preparation for NMR Analysis and Instrumental Methods: 99.96% deuterated D₂O and sodium 3-trimethylsilyl-[2,2,3,3-D₄]propionate (TMSP) were obtained from Aldrich. Other chemicals and biochemicals were of highest quality

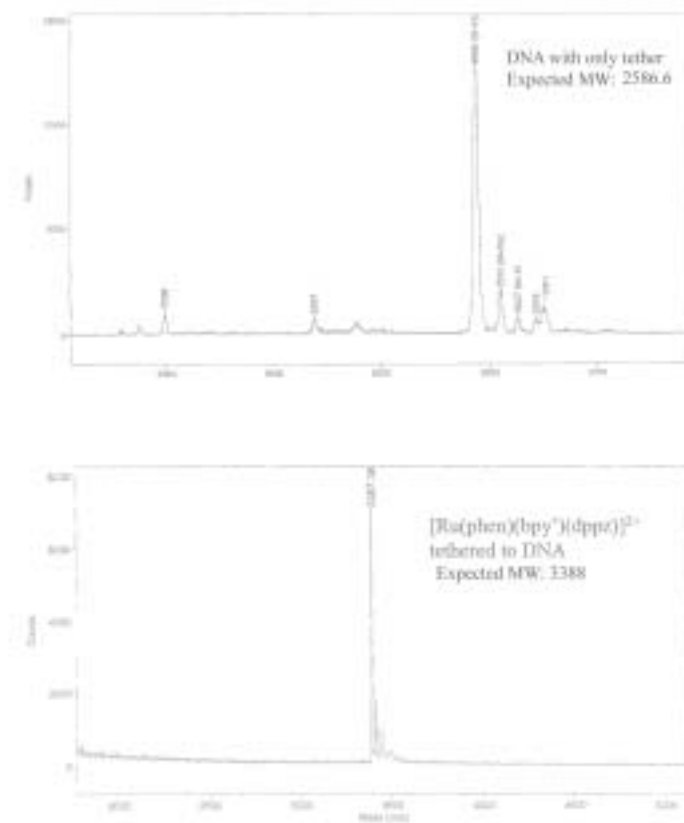


Figure 3.2. The MALDI mass spectrometry of (a) the duplex modified with the nine carbon linker and (b) the duplex tethered to $\text{Ru}(\text{phen})(\text{bpy}')(\text{dppz})^{2+}$.

available commercially. ^1H NMR spectra were recorded in Varian Unity *PLUS*-600 spectrometer with variable temperature control and pulsed-field gradients in three dimensions. For NMR experiments, three oligonucleotide samples each containing the unmodified duplex (a), duplex modified with the nine carbon linker (b) and the duplex tethered to $\text{Ru}(\text{phen})(\text{bpy})(\text{dppz})^{2+}$ (c) were prepared in the following condition: 0.4 mM duplex, 5mM NaCl, 15 mM sodium phosphate, pD 7.0 in 100% D_2O . The chemical shifts are related relative to TMS at 278 K. Samples were repeatedly freeze-dried from D_2O and finally made up in 99.96% D_2O . One-dimensional NMR and NOESY experiments were performed under a series of conditions of temperatures and mixing times to determine the optimum conditions. The conditions used to obtain the best data set are given below. Spectra recorded in D_2O were collected with presaturation of the residual water signal. Typical instrument setting for acquiring one dimensional spectra in D_2O at 600 MHz were as follows: sweep width, 6492 Hz; number of scans, 128; relaxation delay, 1.3s; spectral size, 4416 data points with -0.5 Hz line broadening. Two dimensional phase sensitive NOESY spectra were recorded using 2048 points in t_2 for 512 t_1 values with a mixing time of 150 ms. Highest resolution is achieved at 278 K.

Results

One Dimensional NMR. The one dimensional ^1H NMR spectra of the three samples employed in the experiment are shown in Figure 3. The one dimensional spectrum of the unmodified duplex and the duplex covalently attached with the nine carbon tether were well resolved at 278 K. However, the one dimensional NMR of the duplex tethered to the three ligand complex was broad and characteristic of the binding of the metal complex in fast exchange at the timescale of the NMR. This is consistent with the results obtained from NMR studies of the non-covalently bound $[\text{Ru}(\text{phen})_2\text{dppz}]^{2+}$ complex to DNA (12). It is possible that tethering the metal complex to DNA do not impose any appreciable site specificity.

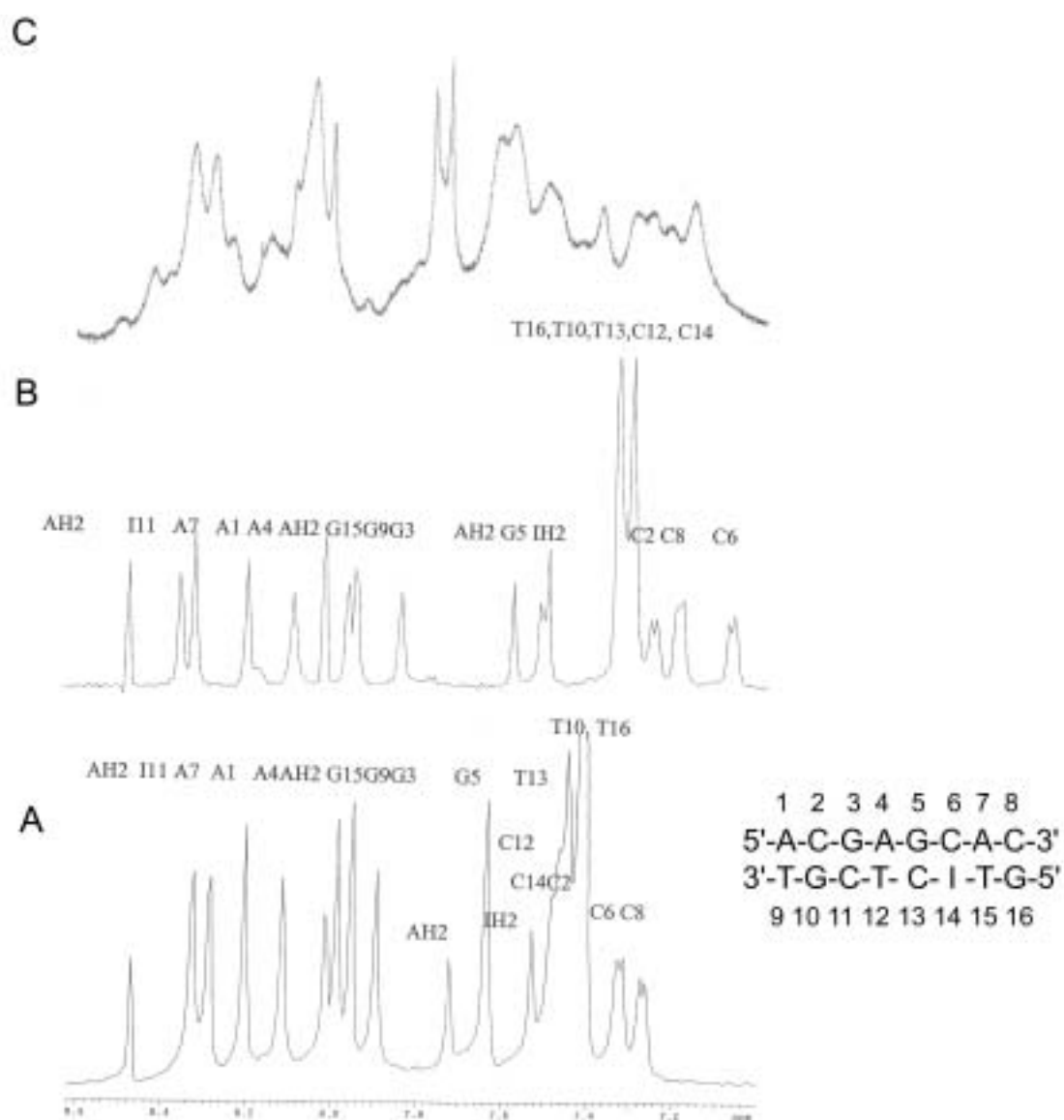


Figure 3.3. ^1H NMR Spectra of (a) the duplex tethered to $\text{Ru}(\text{phen})(\text{bpy}')(\text{dppz})^{2+}$, (b) the duplex modified with the nine carbon linker, and (c) the unmodified duplex. Conditions: 0.4 mM duplex, 5mM NaCl, 15 mM sodium phosphate, 278 K, pD 7.0 in 100% D_2O , Varian UnityPLUS 600 NMR

Two-Dimensional NMR. The spectra of the unmodified duplex and the duplex modified with the tether were assigned from their NOESY spectra assigned by standard techniques (17). In right handed B-DNA duplexes, the base proton (H8 or H6) exhibit NOEs to its own and 5'-flanking sugar H1' and H2'2" protons, allowing an NOE walk from the 5'-to the 3'-end of the oligonucleotide. A clear NOE walk on both the strands was observed in the case of the unmodified duplex identifying the aromatic and sugar H1' protons (Figure 4). A point to note that, the duplex in study is a non self-complementary, hence its assignment involves simultaneous determination of the parallel NOE walks in both the strands. Figure 4 shows the detailed assignment of the aromatic protons of the unmodified duplex.

In case of the duplex modified with the nine carbon tether, clear NOE walk was established in the strand bearing the tether. However, the same cannot be established in case of the opposite strand. The connectivities between 5'-T₁₆-G₁₅-C₁₄-T₁₃-C₁₂-3' were unresolved.

In case of the duplex tethered to the metal complex, very few cross peaks were obtained in the NOESY spectra to make any meaningful assignment and inferences.

Implications

From the limited data collected, not much can be said regarding the binding of the metal complex to the DNA. However, comparing the NOESY spectra of the unmodified duplex and the duplex containing the linker, certain predictions can be made which has bearing on the binding study of the metal complex tethered to DNA by the same ninemer linker. It is apparent from the NOESY spectrum of the duplex containing the tether, that the tether is positioned between the second and fourth bases of the opposite strand where the interaction of the linker with the DNA has resulted in the breaks in NOE connectivities. This region can thus be defined as the "zone" of interaction of the tether with the duplex. The zone is determined by the length and flexibility of the tether. For a

longer linker, possibly the zone is expanded. It is noteworthy that the linker do not interact with the strand of its origin, possibly to avoid high energy conformation to fold back upon the strand of origin.

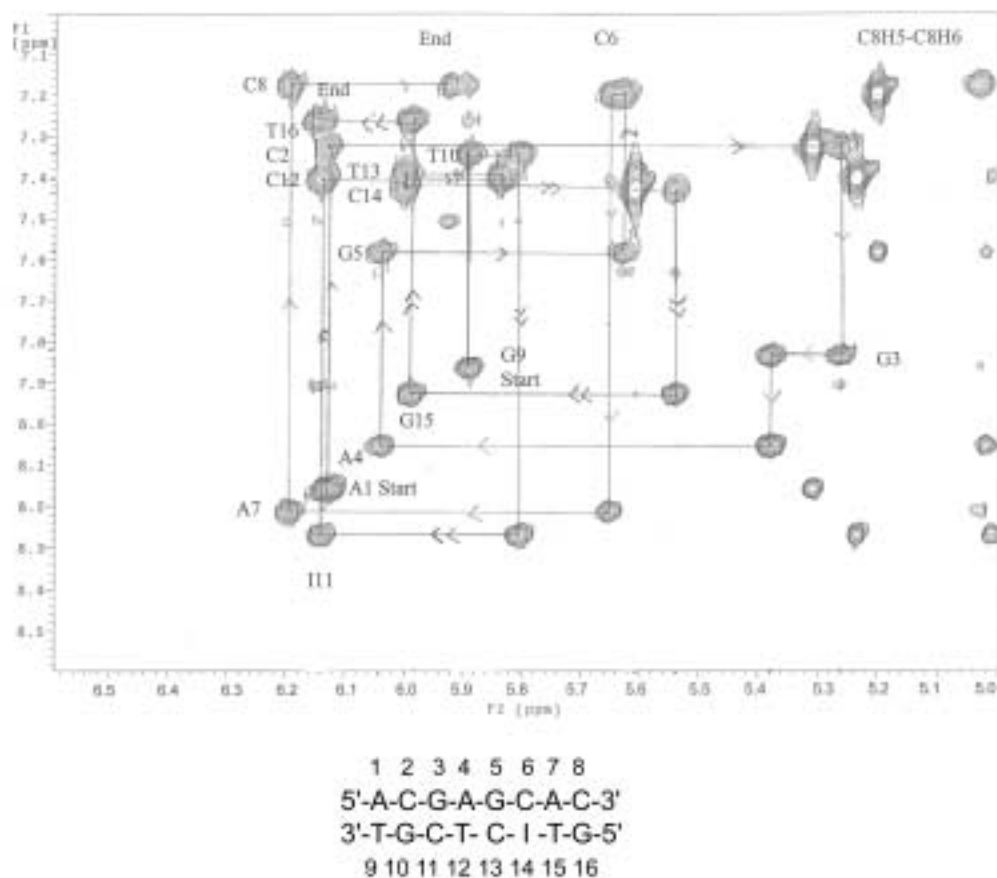


Figure 3.4. Two dimensional ^1H NMR spectra of the free duplex. Shown is a contour plot of the aromatic – sugar H1' region of 150 ms NOESY spectra at 278K. The lines illustrate the NOE walk along the oligonucleotide. Note the two independent NOE walks along the two different strands.

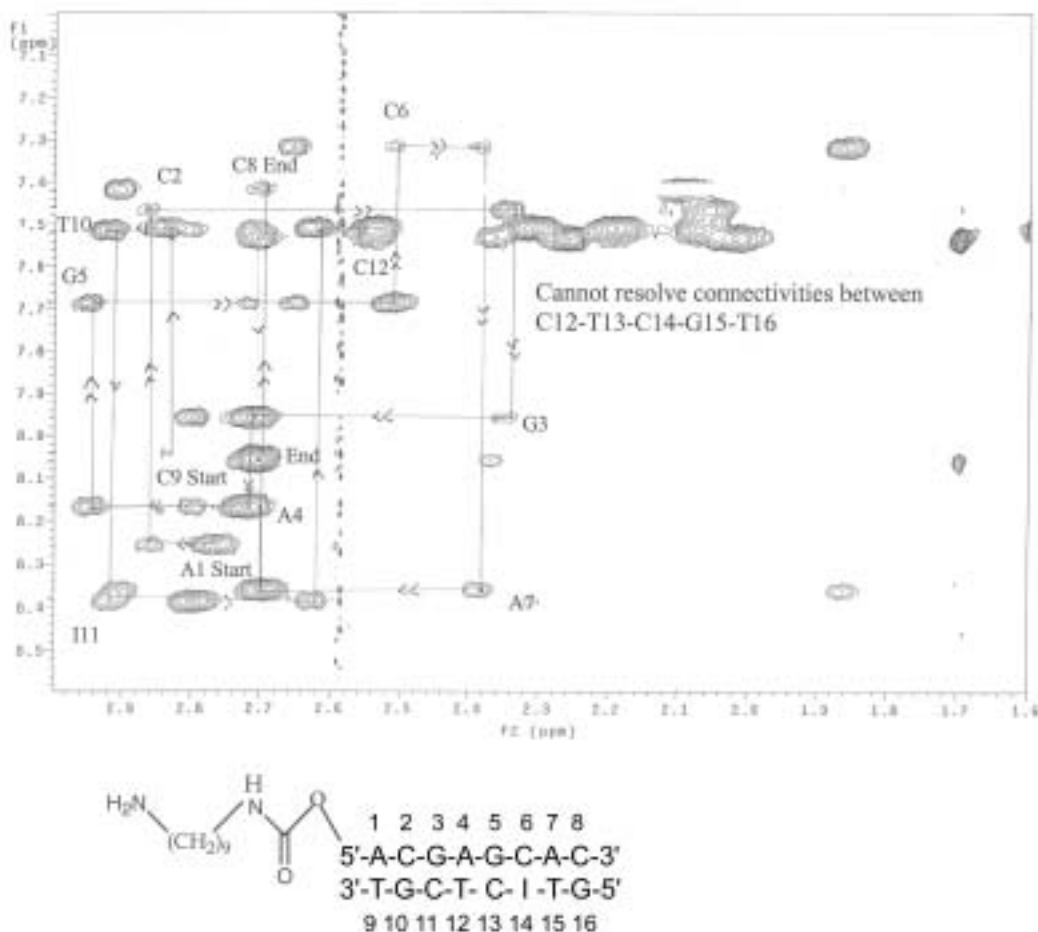


Figure 3.5. Two dimensional ^1H NMR spectra of the duplex with a nine carbon tether. Shown is a contour plot of the aromatic – sugar H2'/H2'' region of 150 ms NOESY spectra at 278K. The lines illustrate the NOE walk along the oligonucleotide. Note the break in the NOE walk in the strand opposite to the linker between C₁₂ and T₁₆ which marks the “zone” of linker interaction

References

1. (a) Murphy, C. J.; Barton, J. K. *Meth. Enzymol.* **1993**, *226*, 570. (b) Turro, N. J.; Tomalia, D. A.; Barton, J. K. *Acc. Chem. Res.* **1991**, *24*, 332.
2. Friedman, A. E.; Chambron, J.-C.; Sauvage, J.-P.; Turro, N. J.; Barton, J. K. *J. Am. Chem. Soc.* **1990**, *112*, 4960.
3. (a) Bannwarth, W.; Schmidt, D.; Stallard, R. L.; Hornung, C.; Knorr, R.; Muller, F. *Helvet. Chim. Acta* **1988**, *71*, 2085. (b) Tessler, J.; Cruickshank, K. A.; Morrison, L. E.; Netzel, T. L.; Chan, C. *J. Am. Chem. Soc.* **1989**, *111*, 7226.
4. (a) Grover, N.; Gupta, N.; Thorp, H. H. *J. Am. Chem. Soc.* **1992**, *114*, 3390. (b) Smith, S. R.; Neyhart, G. A.; Kalsbeck, W. A.; Thorp, H. H. *New J. Chem.* **1992**, *18*, 397.
5. Lecomte, J.-P.; Kirsch- De Mesmaeker, A.; Feeney, M. M.; Kelly, J. M. *Inorg. Chem.* **1995**, *34*, 6481.
6. (a) Jenkins, Y.; Friedman, A. E.; Turro, N. J.; Barton, J. K. *Biochemistry* **1992**, *31*, 10809. (b) Hartshorn, R. M.; Barton, J. K. *J. Am. Chem. Soc.* **1992**, *114*, 5919. (c) Hiort, C.; Lincoln, P.; Norden, B. *J. Am. Chem. Soc.* **1993**, *115*, 3448. (d) Jenkins, Y.; Barton, J. K. *J. Am. Chem. Soc.* **1992**, *114*, 8736.
7. (a) Holmlin, R. E.; Barton, J. K. *Inorg. Chem.* **1995**, *34*, 7. (b) Holmlin, R. E.; Stemp, E. D. A.; Barton, J. K. *J. Am. Chem. Soc.* **1996**, *118*, 5236.
8. Stoeffler, H. D.; Thornton, N. B.; Temkin, S. L.; Schanze, K. S. *J. Am. Chem. Soc.* **1995**, *117*, 7119.
9. Haq, I.; Lincoln, P.; Suh, D.; Norden, B.; Chowdhry, B. Z.; Chaires, J. B. *J. Am. Chem. Soc.* **1995**, *117*, 4788.
10. (a) Yoo, J.; Delaney, S.; Stemp, E.D.A.; Barton, J. K. *J. Am. Chem. Soc.* **2003**, *125*, 6640-6641 (b) Bhattacharya, P.; Barton, J. K. *J. Am. Chem. Soc.* **2001**, *123*, 8649-8656.
11. Turro, C.; Bossmann, S. H.; Jenkins, Y.; Barton, J. K.; Turro, N. J. *J. Am. Chem. Soc.* **1995**, *117*, 9026.
12. (a) Dupureur, C.M.; Barton, J.K. *J. Am. Chem. Soc.* **1994**, *116*, 10286. (b) Dupureur, C.M.; Barton, J.K. *Inorg. Chem.* **1998**, *36*, 33.
13. Caruthers, M. H.; Barone, A. D.; Beaucage, S. L.; Dodds, D. R.; Fisher, E. F.; McBride, L. J.; Matteucci, M.; Stabinsky, Z.; Tang, J. Y. *Methods Enzymol.* **1987**, *154*, 287-313.

14. Anderson, P. A.; Deacon, G. B.; Haarmenn, K. H.; Keene, F. R.; Meyer, T. J.; Reitsma, D. A.; Skelton, B. W.; Strouse, G. F.; Thomas, N. C.; Treadway, J. A.; Whit, A. H. *Inorg. Chem.* **1995**, *34*, 6145.
15. Arkin, M. R.; Stemp, E. D. A.; Barton, J. K. *Chem. Biol.* **1997**, *4*, 389.
16. Dandliker, P. J.; Holmlin, R. E.; Barton, J. K. *Bioconjugate Chem.* **1999**, *10*, 1122.
17. Hudson, B. P.; Dupureur, C. M.; Barton, J. K. *J. Am. Chem. Soc.* **1995**, *117*, 9379.